ChemSusChem

Research Article
doi.org/10.1002/cssc.202400286

Chemistry Europe
European Chemical Societies Publishing

www.chemsuschem.org

Tailoring the Use of 8-Hydroxyquinolines for the Facile Separation of Iron, Dysprosium and Neodymium

Matteo Melegari,[a] Martina Neri,[a] Alex Falco,[a] Matteo Tegoni,[a] Monica Maffini,[a] Fabio Fornari,[a] Claudio Mucchino,[a] Flavia Artizzu,[d] Angela Serpe,*[b, c] and Luciano Marchiò*[a]

Permanent magnets (PMs) containing rare earth elements (REEs) can generate energy in a sustainable manner. With an anticipated tenfold increase in REEs demand by 2050, one of the crucial strategies to meet the demand is developing of efficient recycling methods. NdFeB PMs are the most widely employed, however, the similar chemical properties of Nd (20–30 %wt.) and Dy (0–10 %wt.) make their recycling challenging, but possible using appropriate ligands. In this work, we investigated commercially available 8-hydroxyquinolines (HQs) as potential Fe/Nd/Dy complexing agents enabling metal separation by selective precipitation playing on specific structure/property (solubility) relationship. Specifically, test ethanolic solutions of nitrate salts, prepared to mimic the main components of a PM leachate, were treated with functionalized HQs. We demonstrated that Fe^{3+} can be separated as insoluble $[Fe(Q_{Cl,I})_3]$ from soluble $[REE(Q_{Cl,I})_4]^-$ complexes ($Q_{Cl,I}^-$: 5-Cl-7-I-8-hydoxyquinolinate). Following that, Q_{Cl}^- (5-Cl-8-hydroxyquinolinate) formed insoluble $[Nd_3(Q_{Cl})_9]$ and soluble $(Bu_4N)[Dy(Q_{Cl})_4]$. The process ultimately gave a solution phase containing Dy with only traces of Nd. In a preliminary attempt to assess the potentiality of a low environmental impact process, REEs were recovered as oxalates, while the ligands as well as Bu_4N^+ ions, were regenerated and internally reused, thus contributing to the sustainability of a possible metal recovery process.

Introduction

Developing and adopting sustainable technological processes to extend product life cycles and reduce waste, in line with the objectives of a circular economy model, is a major challenge of our time.[1,2] Neodymium-iron-boron (NdFeB) permanent magnets (PMs) are among the most efficient and widely used magnets on the market. They usually contain Fe (64–69 %), Nd (29–32 %), Dy (1 %) and small amounts of other metals. Their applications are strictly related to the global project referred to as the Ecological Transition since their applications range from hybrid and electric vehicles to wind turbines and solar panels.[3] However, the primary extraction and production of rare earth elements (REEs), pose significant environmental concerns.[4] China dominates global REE production and export, with 44 million metric tons (MT) of reserves, followed by the United States and Australia.[5] However, China's REEs export restrictions in 2010 caused price spikes of REOs and disrupted the global supply chain. As demand for REEs is expected to increase tenfold by 2050 due to the spread of green technologies (as reported by the European Commission forecast), further exacerbating the disparity between the market demand of those critical raw materials and the natural resources of REEs known to be economically feasible for extraction using current technologies.[5,6] For these reasons, the *urban mining* and recycling of REEs from end-of-life appliances, and in particular PMs, are considered among the most appealing potential solutions that the scientific community is being urged to research.[3,7] Direct re-use through application stands as the most favourable way of extending the life span of PMs, mitigating both raw material consumption as well as economic and environmental costs for both new production and treatment of end-of-life PMs. Nevertheless, due to technological constrains, this practice is primarily limited to certain cases, notably large magnets. When the compositions of REE-containing magnets used by different manufacturers are very similar, such as in computer hard disk drives (HDDs), direct utilization through powder processing or by recycling into REE master alloys is feasible.[8,9] Otherwise, the common approach involves separating REEs from transition metals and other elements, such as boron. Recycled REEs mixtures are typically converted

[a] *M. Melegari, Dr. M. Neri, A. Falco, Prof. M. Tegoni, Dr. M. Maffini, Dr. F. Fornari, Prof. C. Mucchino, Prof. L. Marchiò*
Department of Chemistry, Life Sciences and Environmental Sustainability
University of Parma
Parco Area delle Scienze 11/A, 43124, Parma, Italy
E-mail: luciano.marchio@unipr.it

[b] *Prof. A. Serpe*
Department of Civil and Environmental Engineering and Architecture (DICAAR), and Research Unit of INSTM
University of Cagliari
Via Marengo 2, 09123 Cagliari, Italy
E-mail: serpe@unica.it

[c] *Prof. A. Serpe*
Environmental Geology and Geoengineering Institute of the National Research Council (IGAG-CNR)
Piazza d'Armi, 09123 Cagliari, Italy

[d] *Prof. F. Artizzu*
Department of Sustainable Development and Ecological Transition
University of Eastern Piedmont "A. Avogadro"
Piazza S. Eusebio 5, 13100 Vercelli, Italy

Supporting information for this article is available on the WWW under https://doi.org/10.1002/cssc.202400286

into rare earth oxides (REOs), then into new REE alloys for magnet production or other applications. However, industrial recycling of REEs from end-of-life PMs remains significantly low due to the lack of suitable and cost-effective processes. Hence, extensive research efforts have been dedicated to develop new, economically viable and versatile methods for metal separation and recovery from REE-based PMs. A variety of methods have been suggested for recycling REEs from PMs, including hydro-[10](solvo−)[11–13] metallurgical and/or pyrometallurgical routes,[14,15] molten slag methods,[16–18] liquid-liquid[19–24] and gas-phase extraction,[25,26] and more.[27–29] The typical hydrometallurgical approach for recovering materials from $Nd_2Fe_{14}B$ alloys involves the use of strong mineral acids such as HNO_3, HCl, and H_2SO_4, which behave as nonselective leaching agents for pristine alloys as well as thermally oxidized materials.[30,31] The precipitation of iron from acidic leachate by the addition of bases[30,32] is a common practice for separating metals from REEs, however, co-precipitation of REEs is often observed. Other strategies rely on the precipitation of REEs from acidic solutions.[33–36] An alternative approach involves the selective leaching of desired REEs while leaving iron in the residual material.[37–42] The chemical behaviours of iron and REE can be leveraged to effectively separate them from an acidic leachate through selective leaching and/or precipitation methods. However, the separation of neodymium from other REE, such as dysprosium, presents a more challenging task due to their closely resembling chemical properties within the 4f-block of elements.

In industrial settings, conventional liquid−liquid extraction is the most prevalent technique used for this purpose.[19–22] However, these methods require numerous steps to achieve efficient extraction, high consumption of reagents, generation of significant amounts of effluents, and the utilization of harmful and substances.[23,24]

An emerging chemical strategy involves discriminating between REE cations using complexation with specific ligands. By exploiting differences in cation size within the REEs series, complexes with varying nuclearities, hydration numbers, or affinities to supramolecular entities can be formed, resulting in differing solubilities.[43–48] Although the approach is usually limited to the separation of *light* REE (LREE) cations rather than *heavy* REE (HREE) cations, this method offers simplicity and efficiency often achieving high separation factors in a single step, usually in the 100–1000 range for light-heavy REE separation.

In addition to identifying the ideal ligand, the definition of the optimal conditions in terms of metal concentration, additives, pH, solvents, and crystallization conditions are also important for complexation-driven metal separation and recovery.[49] The preference for different coordination numbers (CNs), such as a higher CN for *light* REEs cations than for heavy REEs, as a function of the ionic radius, is a known phenomenon.[50] This behaviour plays a pivotal role in the crystallization of REE inorganic compounds and is functional in REE separation.[51,52]

Ligands of the 8-hydroxyquinoline family have a high affinity for metals comprising NdFeB PMs, giving rise to complexes characterized by different structural features.[53–55] Hence, in this work, we focused on commercially available 8-hydroxyquinoline (HQs) group[56–60] of compounds that act as selective complexing/precipitating agents for the separation of Fe^{3+}, Nd^{3+} and Dy^{3+} in a nonaqueous solvent.

Here, we show how appropriately functionalized 8-hydroxyquinolines in ethanol (listed among the greenest organic solvents)[61] allows for sequential selective precipitation of complexes of three M^{3+} species (Fe, Nd and Dy) from a mixed-metal solution due to differences in the structural features of the products. An Fe, Nd and Dy-nitrate salt solution was selected to mimic leachate from PMs by nonselective treatment with HNO_3.[62] Specifically, when the sterically hindered HQs, are used, the coordination preferences of the three metal cations lead to the formation of the insoluble neutral octahedral iron(III) quinolinolate complex, which precipitates from the solution, against soluble species for both Nd^{3+} and Dy^{3+}. This process accounts for an almost quantitative one-pot Fe/REE separation under mild conditions. Furthermore, when monosubstituted HQ_{Cl} was used, Dy^{3+} and Nd^{3+} formed complexes of different nuclearities as a function of the base employed for the reaction. Indeed, soluble $[Dy(Q_{Cl})_4]^-$ and neutral and almost insoluble $[Nd_3(Q_{Cl})_9]$ complexes were preferentially obtained using Me_4NOH or Bu_4NOH. This peculiar behaviour of the two lanthanides was exploited for Nd/Dy separation. In particular, accurate selection of base and ligand combination allowed us to achieve Nd : Dy separation factors as high as 300, leading to almost pure Dy-oxalate. On these bases, a selective two-step procedure for separating Fe/REE (step 1) and Nd/Dy (step 2) from a mixed-metal ethanol solution is proposed as a possible easy route for recovering metals from waste PM. Furthermore, for circularity considerations, a stepwise procedure allowed for the quantitative recovery of both the HQs utilized in the process and the base precursor for Nd : Dy separation. Overall, the process consumed only nitric acid, oxalic acid and KOH, ultimately affording solid $Fe(OH)_3$ and REE oxalates as the final products.

Results and Discussion

Preliminary Investigation on Iron- and REE-Hydroxyquinoline Complexes

In the initial part of the work, starting from well-known metal complexes already described in the literature, we investigated the behaviour of 8-hydroxyquinoline and its halogen-substituted derivatives as chelating agents for Fe^{3+}, Nd^{3+} and Dy^{3+} ions. The purpose of this preliminary study was to determine the nature of the compounds formed with each synthetic condition and assessing the solubility of the resulting complexes. The conditions that were later chosen for the separation experiments were the ones for which two metals behaved in different ways in terms of solubility. Four 8-hydroxyquinolines where employed for this screening, each one with different steric hindrances on the aromatic ring caused by the presence of halogen functionalizations, ultimately influencing both the

nuclearity and solubility of the complexes in a given solvent. Three quaternary ammonium hydroxides and an aliphatic amine were used as bases to deprotonate the ligand and facilitate the complexation of the metals.

Moreover, when anionic complexes were formed, the cations played an essential role in the ion-pair structure, driving the formation of one type of complex over another and thus further modulating the solubility of the final complex.

Figure 1a summarizes the selected functionalized ligands and bases used in this work. To reasonably simulate the leachate derived from a conventional non-selective hydrometallurgical leaching process on waste PMs, iron and REE nitrates were selected as the inorganic precursors for the study.

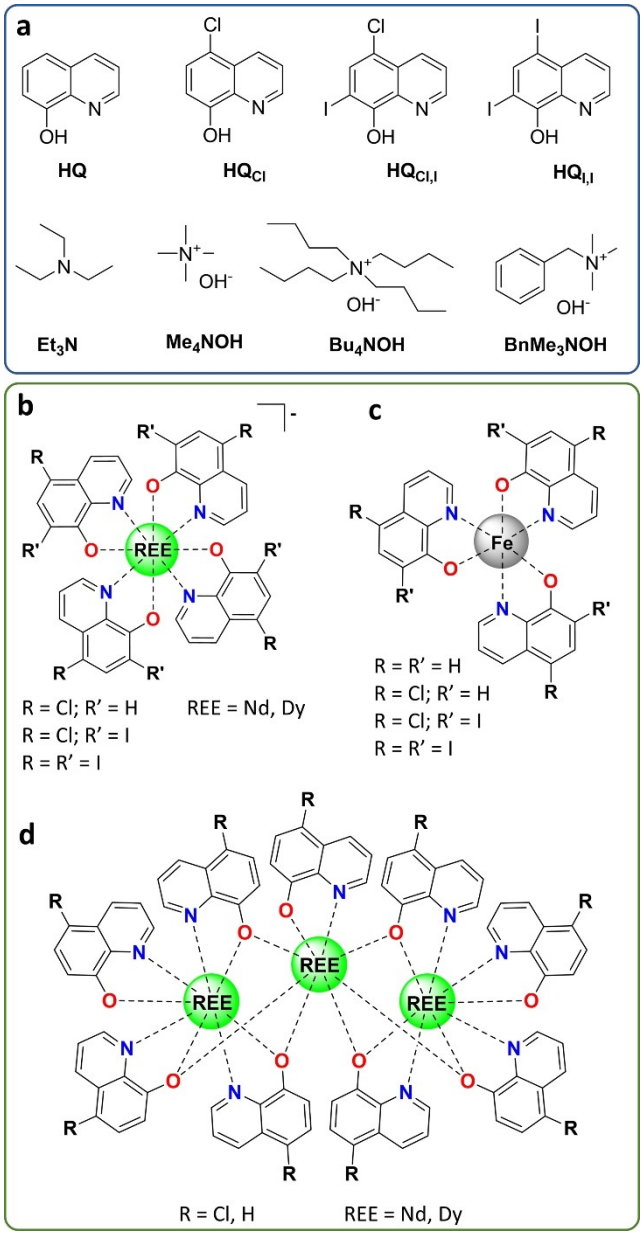

Figure 1. Functionalized 8-hydroxyquinolines and organic bases used in the study (a). Molecular structure of the tetrakis complexes with Nd^{3+} and Dy^{3+} (b). Molecular structures of the Fe^{3+} complexes (c). Molecular structure of the trinuclear complexes with Nd^{3+} and Dy^{3+} (d).

All the reactions were performed in EtOH (THF in the case of $HQ_{I,I}$ due to its poor solubility in EtOH) at 60 °C, systematically varying the hydroxyquinoline and the base for a specific reaction condition. Figure 1b–d summarizes the types of coordination compounds isolated in the solid state and identified as the products of the different syntheses. Generally, we observed the formation of the following: i) tetrakis complex $B[REE(Q_{R,R'})_4]$ (REE was neodymium or dysprosium; $Q_{R,R'}$ was the deprotonated form of the 8-hydroxyquinoline ligand; B^+ was the quaternary ammonium or triethylammonium cation) with more sterically hindered ligands and halogen substituents at both the 5 and 7 positions of the hydroxyquinoline structure ($HQ_{Cl,I}$, $HQ_{I,I}$); ii) insoluble trinuclear complexes $[REE_3(Q_{R,R'})_9]$ and $[REE_3(Q_{R,R'})_8(NO_3)]$, which were formed when unsubstituted and monosubstituted 8-hydroxyquinolines at the 5 position were used (HQ, HQ_{Cl}); and iii) insoluble neutral octahedral $[Fe(Q_{R,R'})_3]$ complexes for all synthetic conditions.[63,64]

Tetrakis-type complexes were consistently isolated with both $HQ_{Cl,I}$ and $HQ_{I,I}$, with no evidence of a behaviour difference for Nd^{3+} and Dy^{3+} since they gave rise to the same type of $B[REE(Q_{R,R'})_4]$ complex under all the conditions explored. In Figure 2, the isolated REE complexes and their solubility in the reaction environment are reported for all the tested conditions. Indeed, it is reasonable to assume that the steric hindrance provided by bulky halogen atoms in position 5 and, even more, in position 7 of the ligands could be the main factor driving the formation of tetrakis complexes with respect to the more crowded trinuclear species. CHN analyses of the resulting compounds generally matched the 4:1 ratio of $HQ_{R,R'}$:REE (see Experimental Section and Tables S4 and S5). In all the cases, mass spectrometry confirmed the presence of tetrakis species (Figures S2–S9), and further confirmation of the formation of $B[REE(Q_{R,R'})_4]$ could be obtained by single-crystal structural analysis (see Supporting Information). Given the differences in the behaviour of REE and Fe^{3+} using $HQ_{Cl,I}$, $HQ_{I,I}$, it was assumed

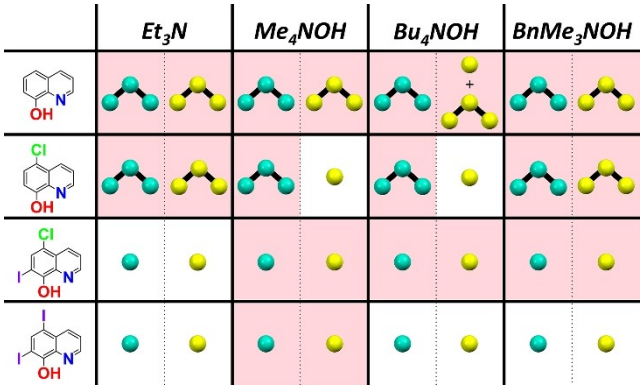

Figure 2. Visual representation of the synthetic conditions used for the preparation of REE-complexes (hydroxyquinoline in row, base in column) and corresponding isolated complexes (● = tetrakis complex for REEs; ●-●-● = trinuclear complex). White and light red backgrounds highlight the conditions in which the complexes are soluble or not completely soluble, respectively, in the reaction environment. For syntheses performed with the same ligand and base, the reactions were performed with the same concentration of Nd^{3+} and Dy^{3+} (range 5–25 mM). Cyan, Nd; Yellow, Dy.

that the separation of REE and Fe^{3+} in those conditions was reasonable and was thus explored (see below).

At the other extreme, when the less hindered HQ and HQ_{Cl} were employed in the synthesis of the complexes, insoluble trinuclear species, namely, $[REE_3(Q_{R,R'})_9]$ and $[REE_3(Q_{R,R'})_8(NO_3)]$, were typically formed (see Experimental Section and Tables S4 and S5) nevertheless with important exceptions. Indeed, while Nd^{3+} always gave the trinuclear system, the Dy^{3+} cation formed the tetrakis species $[Dy(Q_{R,R'})_4]^+$ when using HQ_{Cl}, with Me_4NOH or Bu_4NOH, whereas with HQ and Bu_4NOH, it resulted in a mixture of $(Bu_4N)[Dy(Q)_4]$ (90%) and $[Dy_3Q_9]$ (approximately 10%). The clear formation of different complexes between Dy^{3+} and Nd^{3+} with HQ_{Cl} and Bu_4NOH or Me_4NOH, correlated to the extreme solubility differences of the $(B)[Dy(Q_{Cl})_4]$ (soluble) and $[Nd_3(Q_{Cl})_9]$ (mostly insoluble) complexes, which had important consequences for a possible pathway for REE separation.

Finally, thanks to the high solubilities of the tetrakis complexes, many of the isolated REE-compounds were characterized by single crystal X-ray diffraction. Given the very similar and preserved metal geometries, the structures can be grouped by their different packing motifs and topologies as a function of both the cation and the substituents at the 5 and 7 positions of the hydroxyquinoline moiety (Figure 3). A detailed description of the molecular structures and X-ray data for the complexes reported in this work is provided in the Supporting Information.

Metal Separation from Fe/REE Multimetal Solutions

Selective Iron/REEs Separation

The composition of Nd(Dy)FeB magnets evolves with time by reducing the required amount of Dy in the final functional material.[65] However, the major component in these magnets is iron (approx. 65% by weight), which needs to be separated from the other two elements before attempting intra-series separation. The bulkier hydroxyquinolines $HQ_{Cl,I}$ and $HQ_{I,I}$ formed the tetrakis $[REE(Q_{Cl,I})_4]^-$ or $[REE(Q_{I,I})_4]^-$ anionic species under all the conditions investigated, whereas iron invariably formed the neutral $[Fe(Q_{R,R'})_3]$ complex, which was insoluble in most solvents. Simple reasoning related to the different charges of the two systems drove the separation of iron on one side and Nd/Dy on the other. On the other hand, the lighter quinolines HQ_{Cl} and HQ were not employed for the Fe/REE separation studies because they formed insoluble complexes with one or both REEs, which would likely co-precipitate with the iron complex. We initially determined which of the bases would perform best for this purpose by quantifying the metal content in the supernatant (through ICP-OES) when mixing $HQ_{Cl,I}$ and Nd^{3+} or Fe^{3+} in the presence of different bases. $HQ_{Cl,I}$ was used first as it was soluble in EtOH. Furthermore, only Nd^{3+} was used in those experiments, as the behaviour of Dy^{3+} was presumed to be the same under these conditions. The M:L ratios for these preliminary experiments considered the stoichiometric formation of the $[Fe(Q_{Cl,I})_3]$ and $[Nd(Q_{Cl,I})_4]^-$ complexes.

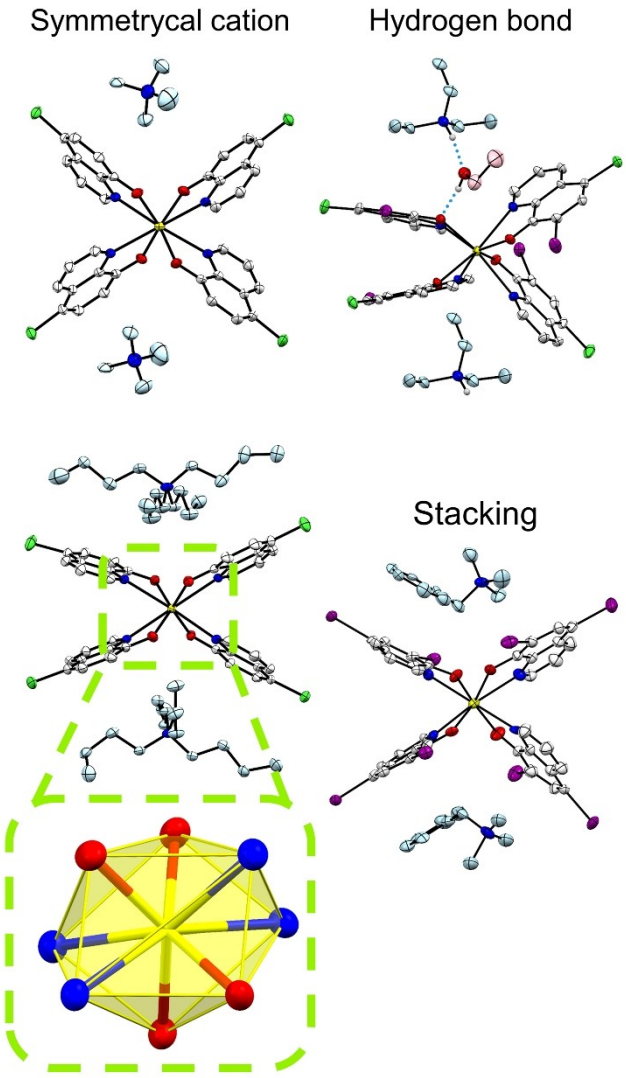

Figure 3. Representation of the different motives in the crystal packings of $[Dy(Q_{R,R'})_4]^-$ complexes with different cations. Two cations are shown for every $[Dy(Q_{R,R'})_4]^-$ structure, even though the anion:cation ratio in the solid state is 1:1. $(Me_4N)[Dy(Q_{Cl})_4]\cdot 2H_2O$ (top left) $(Bu_4N)[Dy(Q_{Cl})_4]\cdot H_2O\cdot 2EtOH$ (bottom left), $(Et_3NH)[Dy(Q_{Cl,I})_4]\cdot EtOH$ (top right) and $(BnMe_3N)[Dy(Q_{I,I})_4]\cdot 0.25THF$ (bottom right). The coordination around the Dy^{3+} ion is highlighted for the structure of $(Bu_4N)[Dy(Q_{Cl})_4]\cdot H_2O\cdot 2EtOH$. Hydrogen bonds between Et_3NH, EtOH and the complex in the structure of $(Et_3NH)[Dy(Q_{Cl,I})_4]\cdot EtOH$ are shown as dotted lines. Atom colors: O, red; N, blue; C, grey (complex)/light blue (cation)/pink (solvent); Dy, yellow; Cl, green; I, purple.

As a result, Et_3N provided the largest difference in solubility between iron and neodymium (Table S6). Et_3N was identified as the best base for use in these experiments because Me_4NOH, Bu_4NOH and $BnMe_3NOH$ led to partial precipitation of the Nd complexes at the same concentration. Once the base was chosen, we then investigated the separation between iron and REEs (one at a time) using $HQ_{Cl,I}$. The amount of ligand used was based on the assumption that $(Et_3NH)[REE(Q_{Cl,I})_4]$ and $[Fe(Q_{Cl,I})_3]$ were the species that formed. During the separation experiments under these reaction conditions, a dark precipitate and a yellow solution were formed for the Fe/Nd and Fe/Dy mixtures. According to the SEM-EDS experiments shown in

Figure 4a–d, the dark solid corresponded to insoluble iron species, whereas the solution contained soluble REE products. According to ICP-OES (inductively coupled plasma optical emission spectroscopy) performed on both the solid and solution phases (2.5 : 2.5 : 2.5 : 27.5 : 27.5 mM of Fe : Nd : Dy : $HQ_{Cl,I}$: NEt_3) all of the iron was precipitated, leaving only the REE complexes in the solution phase. The solid phase showed the presence of a minimal amount of Dy and Nd (5% and 4% of the total amount of the metals, respectively) most likely due to a concomitant precipitation of REE complexes together with the iron complex. The separation factors between Fe and Nd and between Fe and Dy were > 1800 and > 1400, respectively (Table 1).

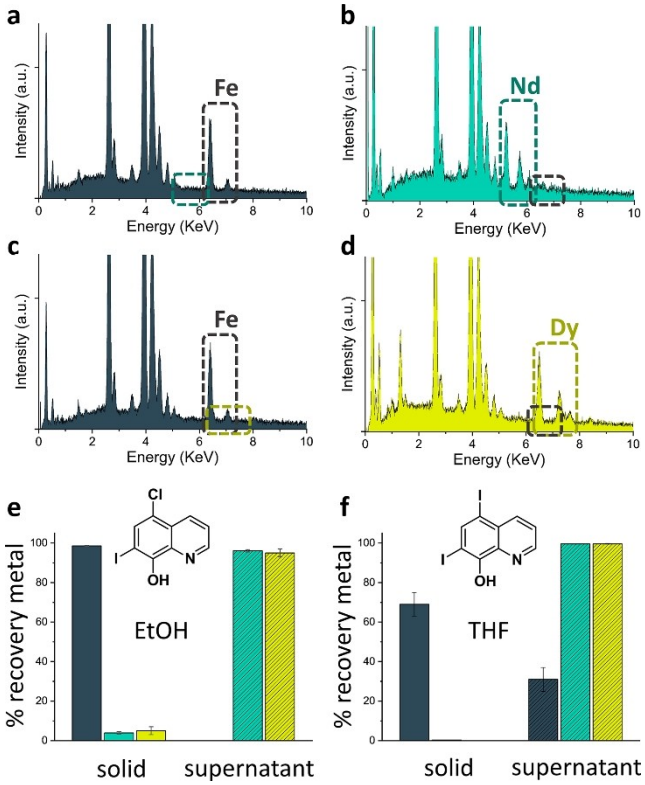

Figure 4. EDS spectra obtained from the precipitated solid (a) and from the dried supernatant (b) in EtOH when using $HQ_{Cl,I}$/Et_3N and a 1 : 1 mixture of $Fe(NO_3)_3 \cdot 9H_2O$ and $Nd(NO_3)_3 \cdot 6H_2O$. EDS spectra obtained from the precipitated solid (c) and from the dried supernatant (d) in EtOH when using $HQ_{Cl,I}$/Et_3N and a 1 : 1 mixture of $Fe(NO_3)_3 \cdot 9H_2O$ and $Dy(NO_3)_3 \cdot 6H_2O$. ICP-OES analysis performed on the solution and solid phases for the systems comprising a 1 : 1 : 1 mixture of $Fe(NO_3)_3 \cdot 9H_2O$ and $Nd(NO_3)_3 \cdot 6H_2O$ and $Dy(NO_3)_3 \cdot 6H_2O$ in presence of $HQ_{Cl,I}$/Et_3N (EtOH as solvent) (e) and $HQ_{I,I}$/Et_3N (THF as solvent) (f); results are reported as mean ± standard deviation.

For the sake of completeness, we performed the same type of experiments with the bulkier and more lipophilic $HQ_{I,I}$ ligand, even though the solvent needed for the separation was nongreen THF due to the poor solubility of the ligand in EtOH. From the ICP-OES data, it was evident that the complex $[Fe(Q_{I,I})_3]$ was partly soluble under the investigated conditions, and a significant amount of iron was found in the solution phase together with the $[REE(Q_{I,I})_4]^-$ species (approximately 30% of the starting iron).

Hence, we identified $HQ_{Cl,I}$ in the presence of Et_3N as the ideal condition for separating iron from a Nd/Dy mixture from a 1 : 1 : 1 metal mixture.

Iron can be recovered from an $[Fe(Q_{Cl,I})_3]$ ethanol mixture by adding KOH. After drying and neutralization of the supernatant with 1 M HNO_3, insoluble $Fe(OH)_3$ and pure $HQ_{Cl,I}$ were obtained.[66] $(Et_3NH)[REE(Q_{Cl,I})_4]$ were then treated with nitric acid in water, leading to the formation of soluble REE-nitrates and $HQ_{Cl,I}$, which can then be separated by centrifugation due to their low solubility in aqueous media. The recovery of $HQ_{Cl,I}$ from the Fe complex and from the REE complexes was 85% and quantitative, respectively, leading to an overall recovery yield of 93%, thus increasing the sustainability of the process. Ultimately, the separation provided $REE(NO_3)_3$ as a product that can be used as the starting point for the second separation step; conversely, common methods of iron/REE separation lead to REE oxalates as products, necessitating an intermediate calcination step.[33]

Selective Nd/Dy Separation

A more challenging task was to achieve efficient separation between Nd^{3+} and Dy^{3+}. Hence, we chose HQ_{Cl}, which was able to provide the best differential solubility for Nd^{3+} and Dy^{3+} complexes. According to the experimental observations derived from the structural analysis, different Nd^{3+} and Dy^{3+} systems characterized by different solubilities in ethanol were expected when using HQ_{Cl}. As in the previous separation experiments, we used metal nitrates at a 1 : 1 ratio (10 mM) in ethanol. The stoichiometric M : L ratio was based on the assumption that $[Dy(Q_{Cl})_4]^-$ and $[Nd_3(Q_{Cl})_9]$ were preferentially formed on account of the structural analysis described above. All four bases were tested in these preliminary experiments even though Me_4NOH and Bu_4NOH were the only bases that provided different solubilities to the Nd and Dy complexes in the single-metal experiments reported above. The physical separation between the solid and the solution phase was performed after 1 h of

Table 1. Separation coefficients (S) and enrichment factors (EFs) for the separations of iron and REEs. The results are reported as the mean ± standard deviation, rounded at one significant digit. For the experiments in which the concentration of one of the metals was < LOQ (limit of quantification), the standard deviation value was not reported.

$HQ_{R,R'}$	Base	$EF_{Fe/Nd,solid}$	$EF_{Fe/Dy,solid}$	$EF_{Nd,supernatant}$	$EF_{Dy,supernatant}$	$S_{Fe/Nd}$	$S_{Fe/Dy}$
$HQ_{Cl,I}$	**Et_3N**	**27 (±5)**	**20 (±10)**	**> 70**	**> 70**	**> 1800**	**> 1400**
$HQ_{I,I}$	Et_3N	> 190	> 240	3.2 (±0.6)	3.0 (±0.4)	> 610	> 720

$EF_{M1/M2} = n_{M1}/n_{M2}$, where n is the number of moles; $S_{M1/M2} = EF_{M1/M2,solid} \cdot EF_{M2/M1,supernatant}$.

mixing the reagents at 60 °C. Initially, we roughly assessed the metal composition of the precipitate (wt.%) using SEM-EDS (Figure 5). The four organic bases had an important influence on the outcome of the precipitation. Unsurprisingly, in the presence of Et_3N and $BnMe_3NOH$, there was no selective precipitation of one of the two metals, whereas in the presence of Me_4NOH and Bu_4NOH, the solid was significantly enriched in Nd, consequently concentrating the solution in Dy. The two metal cations in the presence of HQ_{Cl} and Me_4NOH or Bu_4NOH were then quantified via ICP−OES analysis (Table 2). In general, when starting from a 1:1 Nd^{3+}/Dy^{3+} mixture, the solid precipitate contained most of the Nd initially used and a variable amount of Dy ranging from 15 to 40% with respect to the initial quantity.

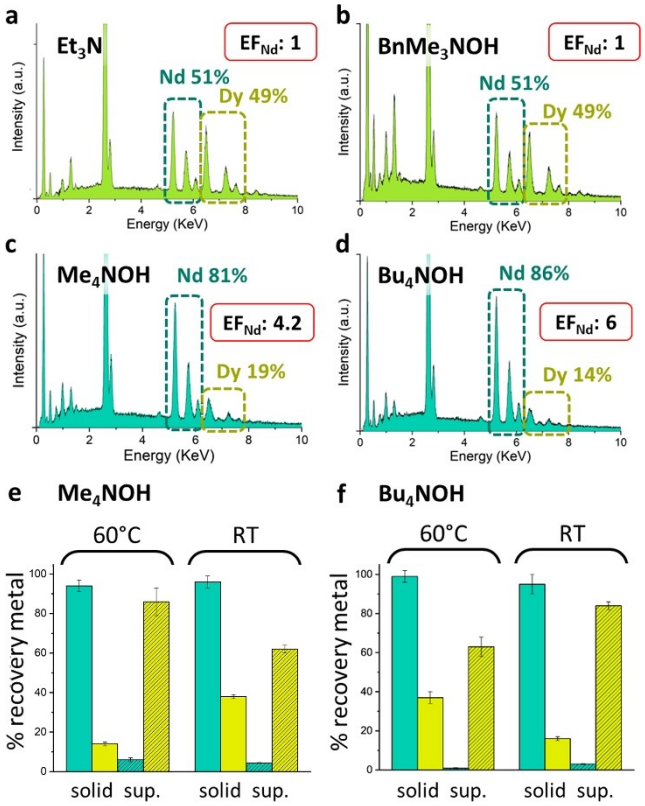

Figure 5. EDX spectra obtained from the precipitated solid in EtOH when using HQ_{Cl}/Et_3N (a), $HQ_{Cl}/BnMe_3NOH$ (b), HQ_{Cl}/Me_4NOH (c) and HQ_{Cl}/Bu_4NOH (d), and a 1:1 mixture of $Nd(NO_3)_3\cdot 6H_2O$ and $Dy(NO_3)_3\cdot 6H_2O$. ICP-OES analysis performed on the solution and solid phases for the systems comprising a 1:1 mixture of $Nd(NO_3)_3\cdot 6H_2O$ and $Dy(NO_3)_3\cdot 6H_2O$ in EtOH, in presence of HQ_{Cl}/Me_4NOH (e) and HQ_{Cl}/Bu_4NOH (f), at 60 °C or at room temperature; results are reported as mean ± standard deviation.

Most importantly, the solution phase was almost pure in Dy (purity *ca.* 99% for the experiment with Bu_4NOH). The S and EF parameters are reported in Table 2 (all conditions reported in the Supporting Information). Additional experiments were also performed to test the less promising HQ. Not surprisingly, the metals behaved in similar ways, resulting in unsatisfactory enrichment and separation factors (Table S10).

Finally, to better simulate a real NdFeB system, separation experiments with HQ_{Cl} were performed using different Nd:Dy ratios (4:1, 9:1 and 30:1, ratio found in permanent magnets), maintaining a 10 mM concentration of Nd^{3+}. Under all tested conditions, Bu_4NOH performed better than Me_4NOH, leading to greater separation factors. This can be explained by the greater surface area of the Bu_4N^+ cation with respect to that of the Me_4N^+ cation, which leads to greater interactions with the negatively charged tetrakis complex. With Bu_4NOH, the $S_{Nd/Dy}$ values were 180 (Nd:Dy 1:1), 120 (Nd:Dy 4:1), 70 (Nd:Dy 9:1) and 130 (Nd:Dy 30:1), indicating that the procedure can potentially be applied to a real PM sample while retaining a high separation factor. Additional experiments were performed with a higher percentage of Dy^{3+} than Nd^{3+} to simulate a possible second treatment of the separation leachate, which was rich in Dy^{3+}. To do so, we used starting ratios of Nd:Dy of 1:4 and 1:9. For the former experiment, an efficient separation was retained (S = 100); however, for the latter experiment, the small amount of Nd^{3+} prevented the precipitation of the complex, leading to unsuccessful separation.

At the end of the separation trials, HQ_{Cl} was recovered from both the isolated $(Bu_4N)[Dy(Q_{Cl})_4]$ and $[Nd_3(Q_{Cl})_9]$ after treatment with oxalic acid in water at 60 °C, leading to the formation of insoluble $REE_2(C_2O_4)_3$ octa/nonahydrate[67] and partially soluble $[H_2Q_{Cl}]_2[oxalate]\cdot 2H_2O$, which was dissolved in ethanol and separated from the metal salts. The ligand was recovered from the supernatant and treated with the minimum amount of potassium hydroxide in water (0.1 M) up to a pH of 6, leading

Table 2. Separation coefficients and enrichment factors for the intra-series separations of neodymium and dysprosium under the indicated conditions. The two best conditions for the separation are reported in bold. The results are reported as the mean ± standard deviation, rounded at one significant digit (replicate).

Base	Nd:Dy ratio	$EF_{Nd,solid}$	$EF_{Dy,supernatant}$	$S_{Nd/Dy}$	% Recovery of Dy	% Purity of Dy
Me_4NOH	1:1	6.7 (±0.6)	14 (±2)	90 (±10)	86 (±7)	93.3
Bu_4NOH	**1:1**	**2.6 (±0.3)**	**70 (±10)**	**180 (±40)**	**63 (±5)**	**98.6**
	4:1	7.1 (±0.3)	17 (±4)	120 (±30)	45 (±1)	94.4
	9:1	9.0 (±0.4)	>8.1	>70	18.8 (±0.6)	89.0
	30:1	33 (±2)	4 (±1)	130 (±40)	12.3 (±0.1)	80.0
	1:4	7 (±1)	14 (±5)	100 (±40)	97 (±7)	93.3
KOH + Bu_4NOH	**1:1**	**3 (±2)**	**130 (±30)**	**300 (±100)**	**76 (±5)**	**99.2**

$EF_{M1} = n_{M1}/n_{M2}$, where n is the number of moles; $S_{M1/M2} = EF_{M1/M2, solid} \cdot EF_{M2/M1, supernatant}$; % recovery of $Dy = n_{Dy, supernatant}$ (found)/$n_{Dy, starting} \cdot 100$; % purity of $Dy = n_{Dy, supernatant}/(n_{Dy,supernatant} + n_{Nd,supernatant}) \cdot 100$.

to the precipitation of pure HQ_{Cl}. The total recovery efficiency of HQ_{Cl} was >95% (Figure 6).

The recovery of the Bu_4N^+ cation in the form of $(Bu_4N)NO_3$ was achieved after drying the aqueous supernatant phase of the HQ_{Cl} recovery experiments from the Dy^{3+} complex and washing it with the minimal amount of EtOH.

As a proof of concept, separation of the 1:1 system was also attempted using KOH as the base (6 equivalents) and Bu_4NOH (1 equivalent) as the quaternary ammonium ion source. The results of the separation experiments proved to be outstanding, with a final separation factor of 300 and a Dy^{3+} purity of 99.2% in the supernatant. Additional experiments carried out using KOH (7 equivalents) and $(Bu_4N)NO_3$ (1 equivalent) proved to be less effective; nonetheless, these materials retained a good separation factor of 70. These final experiments showed that the role of tetrabutylammonium salt/hydroxide is mainly to provide Bu_4N^+ cations for the stabilization of the tetrakis Dy^{3+} complex.

Preliminary Considerations about the Potential Application and Environmental Impact

To preliminarily investigate the potential appeal of the proposed method for practical application, we considered several hazards related to the use of the selected reagents and solvents as well as the "greenness" of the chemical approach.[68–70] Specifically, Figure S38 summarizes the hazard indications for the reagents and solvents used in this work. Although further efforts are required to validate an applicative model based on the proposed method, a potentially suitable configuration for sequential metal recovery was designed by considering both the safety perspective and the high efficiency of separation (Figure 6). As shown, the recovery process involved only ethanol and water as solvents, avoiding the use of solvents with a penalty higher than 2. The ligand used for REE separation, HQ_{Cl}, is a non-hazardous, commercially available, and economically affordable reagent that can be recovered in up to 95 wt.% yield. On the other hand, the best selectivity for Fe/REE separation was obtained with $HQ_{Cl,I}$, which

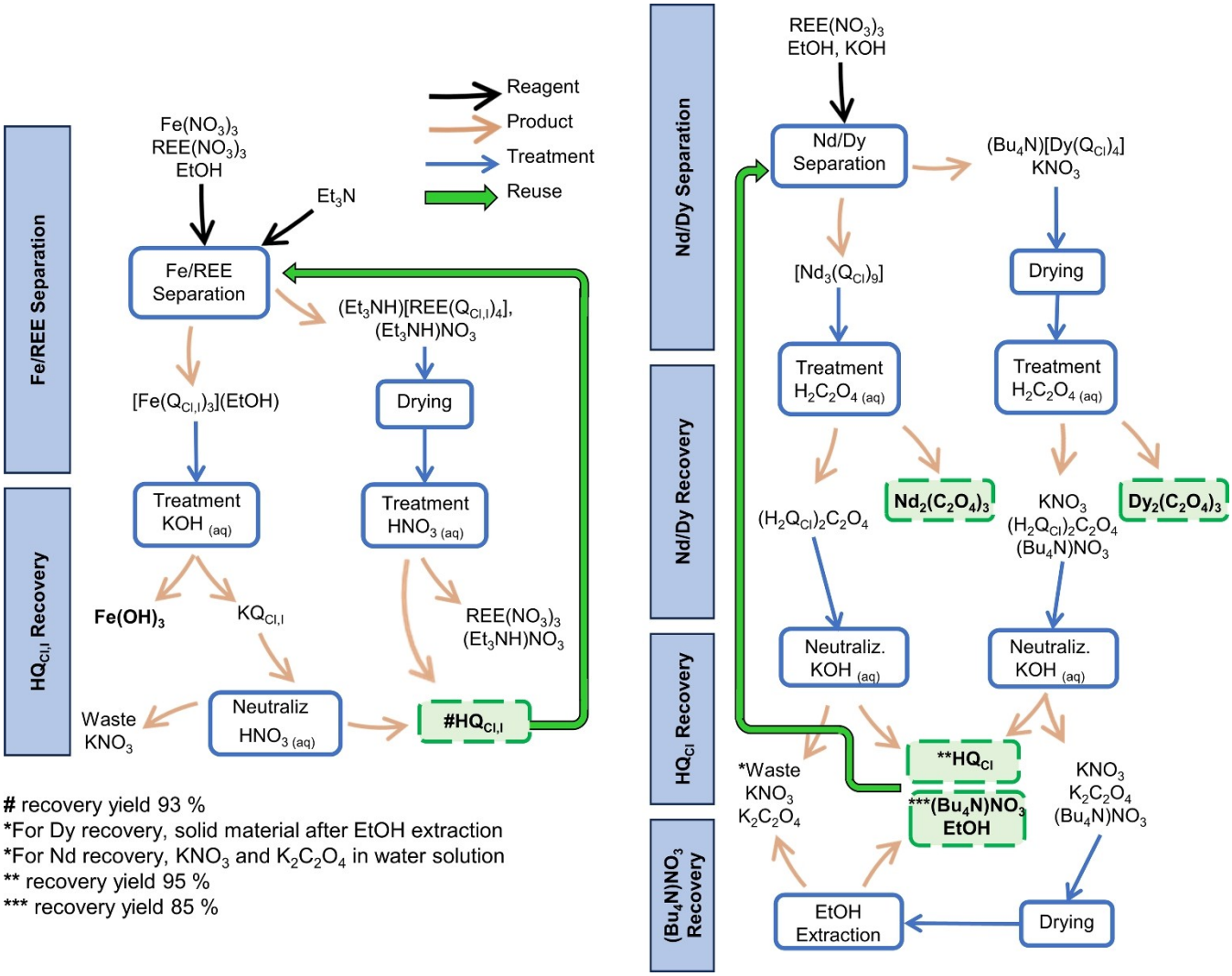

Figure 6. General scheme describing the steps for the sequential separation of the metals from a 1:1:1 $Fe^{3+}/Nd^{3+}/Dy^{3+}$ mixture using $HQ_{Cl,I}/Et_3N$ (left) and the separation of Nd^{3+}/Dy^{3+} from a 1:1 mixture using $HQ_{Cl}/KOH/Bu_4NOH$ (right) together with the $HQ_{Cl,I}$, HQ_{Cl} and Bu_4N^+ recovery percentages.

is currently used under the name Clioquinol as an antifungal agent for topical application.[71] Due to the high degree of recyclability of the reagents and solvents, the process consumed only oxalic acid, nitric acid, KOH, and NEt_3, as it was possible to recover both ligands and $(Bu_4N)NO_3$ after Nd/Dy separation. We were able to recover Fe and REEs in high yield and good purity by exploiting two one-pot and straightforward separation steps (Figure S37). Bu_4NOH was the best choice compared to Me_4NOH, both from a safety perspective (Figure S38 and Table S25) and from the efficiency of the separation process. Based on the process scheme and detailed experimental data, the most representative green chemistry metrics for the specific system were estimated and are summarized in Table S26.

Important information was provided by the mass productivity (MP), which highlighted the percentage of valorised material in the leaching process. The use of a nonwatery medium heavily affected the MP. Notably, EtOH is an environmentally sustainable solvent (listed among the most sustainable green solvents) and is fully recyclable, mitigating wastewater production. On the other hand, the E factor (EF) may represent a good connection between the laboratory and the industrial scale. Indeed, the EF correlates the amount of desired products with that of generated waste.

The reported EF values for the Fe separation indicated that this step made the most significant contributions to waste production in the designed process. According to the effective mass yield (EMY) parameter, Fe separation and recovery also represented the least safe phase of the process due to the use of an acute toxicity reagent.

Although more quantitative information can be obtained from a life cycle assessment on a consolidated process scheme, we can preliminarily state that the separation of iron did not seem as green as the intra-series Nd/Dy separation, as both the hydroxyquinolines and the base used are associated with a higher hazard degree, and the metrics are less favourable. For this reason, despite the interesting and very selective behaviour shown by $HQ_{Cl,I}$ for Fe/REE separation, other more sustainable reagents may be used for this purpose. In contrast, Nd/Dy separation under the reported conditions seemed particularly appealing because of the high level of separation in just one pot achieved by using eco-friendly reagents under mild conditions (60 °C, 1 h) and because of the almost quantitative recycling of ethanol, ligands and cation sources. The only reagents that are consumed in the Nd/Dy separation process are KOH, HNO_3 and $H_2C_2O_4$, which are all widely available and inexpensive (a detailed description of the process is reported in Figure S37).

Conclusions

In recent years, the demand for REEs has grown significantly, and efforts have been directed toward the development of environmentally friendly methods for their recovery from electronic waste. Today, the amount of recovered REEs corresponds to only 5% by weight of the total industry demand. It is therefore important to increase the percentage of recycling and REEs recovery from waste, possibly generating high-value products. In this work, we used nitrate solutions of iron and REEs (Nd and Dy) as starting material for the separation trials. We investigated stepwise methods that allowed the separation or enrichment of singular metals starting from Fe/Nd/Dy mixtures using known and commercially available systems such as hydroxyquinolines and quaternary ammonium hydroxides or triethylamine. The use of negatively charged ligands and their bidentate nature led to different stoichiometries and therefore different net charges for the iron and REE complexes owing to their different coordination preferences. Indeed, this separation was straightforward, with a minimal quantity of Fe left in solution (<1%). The ligand can be recovered from the iron complex, whereas REE complexes can regenerate the ligand by direct treatment with nitric acid in water. The REE nitrate could then be considered as the primary materials for subsequent processing aimed at addressing the Nd/Dy separation. The ligand HQ_{Cl} preferentially formed neutral trinuclear complexes with Nd but charged mononuclear complexes with Dy, using certain bases, thanks to the minimal but significant difference in their ionic radii. In particular, Bu_4NOH gave a separation factor of approximately 180. Even though the solid phase was enriched with Nd but with a consistent amount of Dy, the solution phase contained almost exclusively Dy. HQ_{Cl} could be completely recovered by treatment with oxalic acid, providing REE oxalate, which could eventually be thermally decomposed to the corresponding oxides.[38,67,72] The Bu_4N^+ cation could also be recovered from the Dy-enriched supernatant as $(Bu_4N)NO_3$. Finally, the use of KOH together with Bu_4NOH gave an outstandingly high separation factor of 300 with a final Dy purity of 99.2%. The method described provides insights into the factors governing the separation and recovery of metals using low-denticity ligands via a green chemistry approach, with high sustainability potential due to the recovery of most valuable reagents.

Supporting Information

List of the abbreviations; statistical analysis on CCDC structures; Experimental Section; Separation studies; Description of the X-ray molecular structures; process scheme; evaluation of selected environmental parameters. Deposition Numbers 2270899–2270913 contain the supplementary crystallographic data for this paper. These data are provided free of charge by the joint Cambridge Crystallographic Data Centre and Fachinformationszentrum Karlsruhe Access Structures service. The authors have cited additional references within the Supporting Information (Ref. [73–103]).

Acknowledgements

This work benefited from the equipment and framework of the COMP-R Initiative, funded by the "Departments of Excellence" program of the Italian Ministry for Education, University and

Research (MIUR, 2023–2027). Chiesi Farmaceutici SpA is acknowledged for the support of the D8 Venture X-ray equipment. This work has been supported by the project "Green processes for Rare Earth Elements Separation, recovery & valorization from permanent Magnets (GREEn SM)" funded by the MUR PRIN: progetti di ricerca di rilevante interesse nazionale 2022, grant number 2022T3H2CW. Open Access publishing facilitated by Università degli Studi di Parma, as part of the Wiley - CRUI-CARE agreement.

Conflict of Interests

The authors declare no conflict of interest.

Data Availability Statement

The data that support the findings of this study are available from the corresponding author upon reasonable request.

Keywords: Rare Eart Elements · REEs Separation · Neodymium Magnets · Sustainability · Recycling

[1] European Commision, *New Circular Economy Action Plan (CEAP)*, **2020**, 1–19.
[2] R. Galvin, N. Healy, *Energy Res. Soc. Sci.* **2020**, *67*, 101529.
[3] Y. Yang, A. Walton, R. Sheridan, K. Güth, R. Gauß, O. Gutfleisch, M. Buchert, B.-M. Steenari, T. Van Gerven, P. T. Jones, K. Binnemans, *J. Sustain. Metall.* **2017**, *3*, 122–149.
[4] C. Hurst, *China's Rare Earth Elements Industry: What Can the West Learn?*, **2010**, 1–42.
[5] U. S. Geological Survey, *Mineral Commodity Summaries* **2022**, 2022, 134–135.
[6] E. Sme, *Study on the Critical Raw Materials for the EU*, **2023**, 1–152.
[7] J. H. Rademaker, R. Kleijn, Y. Yang, *Environ. Sci. Technol.* **2013**, *47*, 10129–10136.
[8] M. Zakotnik, I. R. Harris, A. J. Williams, *J. Alloys Compd.* **2008**, *450*, 525–531.
[9] A. Walton, H. Yi, N. A. Rowson, J. D. Speight, V. S. J. Mann, R. S. Sheridan, A. Bradshaw, I. R. Harris, A. J. Williams, *J. Cleaner Prod.* **2015**, *104*, 236–241.
[10] A. Akcil, Y. A. Ibrahim, P. Meshram, S. Panda, *J. Chem. Technol. Biotechnol.* **2021**, *96*, 1785–1797.
[11] M. Orefice, K. Binnemans, *Sep. Purif. Technol.* **2021**, *258*, 117800.
[12] N. K. Batchu, B. Dewulf, S. Riaño, K. Binnemans, *Sep. Purif. Technol.* **2020**, *235*, 116193.
[13] B. Dewulf, N. K. Batchu, K. Binnemans, *ACS Sustainable Chem. Eng.* **2020**, *8*, 19032–19039.
[14] M. Firdaus, M. A. Rhamdhani, Y. Durandet, W. J. Rankin, K. McGregor, *J. Sustain. Metall.* **2016**, *2*, 276–295.
[15] Y.-Y. Bian, S.-Q. Guo, Y.-L. Xu, K. Tang, X.-G. Lu, W.-Z. Ding, *Rare Met.* **2022**, *41*, 1697–1702.
[16] T. Saito, H. Sato, S. Ozawa, J. Yu, T. Motegi, *J. Alloys Compd.* **2003**, *353*, 189–193.
[17] Y. Yang, S. Abrahami, Y. Xiao, in *3rd Int. Slag Valoris. Symp.*, **2013**, pp. 249–252.
[18] M. Tanaka, T. Oki, K. Koyama, H. Narita, T. Oishi, in *Handb. Phys. Chem. Rare Earths*, Elsevier B. V., **2013**, pp. 159–211.
[19] E. O. Opare, E. Struhs, A. Mirkouei, *Renewable Sustainable Energy Rev.* **2021**, *143*, 110917.
[20] Y. A. El-Nadi, *Sep. Purif. Rev.* **2017**, *46*, 195–215.
[21] T. Dizhbite, G. Zakis, A. Kizima, E. Lazareva, G. Rossinskaya, V. Jurkjane, G. Telysheva, U. Viesturs, *Bioresour. Technol.* **1999**, *67*, 221–228.
[22] K. R. Johnson, D. M. Driscoll, J. T. Damron, A. S. Ivanov, S. Jansone-Popova, *JACS Au* **2023**, *3*, 584–591.
[23] M. C. Bonfante, J. P. Raspini, I. B. Fernandes, S. Fernandes, L. M. S. Campos, O. E. Alarcon, *Renewable Sustainable Energy Rev.* **2021**, *137*, 110616.
[24] E. Vahidi, F. Zhao, *J. Environ. Manage.* **2017**, *203*, 255–263.
[25] K. Miura, M. Itoh, K.-I. Machida, *J. Alloys Compd.* **2008**, *466*, 228–232.
[26] K. Murase, K. Shinozaki, Y. Hirashima, K. Machida, G. Adachi, *J. Alloys Compd.* **1993**, *198*, 31–38.
[27] Z. Chen, Z. Li, J. Chen, P. Kallem, F. Banat, H. Qiu, *J. Environ. Chem. Eng.* **2022**, *10*, 107104.
[28] Y. Zhang, F. Gu, Z. Su, S. Liu, C. Anderson, T. Jiang, *Metals (Basel).* **2020**, *10*, 841.
[29] K. Binnemans, P. T. Jones, B. Blanpain, T. Van Gerven, Y. Yang, A. Walton, M. Buchert, *J. Cleaner Prod.* **2013**, *51*, 1–22.
[30] O. Dudarko, N. Kobylinska, V. Kessler, G. Seisenbaeva, *Hydrometallurgy* **2022**, *210*, 105855.
[31] E. Emil-Kaya, B. Polat, S. Stopic, S. Gürmen, B. Friedrich, *RSC Adv.* **2023**, *13*, 1320–1332.
[32] M. A. R. Önal, C. R. Borra, M. Guo, B. Blanpain, T. Van Gerven, *J. Rare Earth* **2017**, *35*, 574–584.
[33] F. Liu, C. Peng, B. P. Wilson, M. Lundström, *ACS Sustainable Chem. Eng.* **2019**, *7*, 17372–17378.
[34] T. Itakura, R. Sasai, H. Itoh, *J. Alloys Compd.* **2006**, *408–412*, 1382–1385.
[35] E. Yamada, H. Murakami, S. Nishihama, K. Yoshizuka, *Sep. Purif. Technol.* **2018**, *192*, 62–68.
[36] J. Niskanen, M. Lahtinen, S. Perämäki, *Clean. Eng. Technol.* **2022**, *10*, 100544.
[37] C. Liu, Q. Yan, X. Zhang, L. Lei, C. Xiao, *Environ. Sci. Technol.* **2020**, *54*, 10370–10379.
[38] T. Vander Hoogerstraete, B. Blanpain, T. Van Gerven, K. Binnemans, *RSC Adv.* **2014**, *4*, 64099–64111.
[39] J. J. Heckman, R. Pinto, P. A. Savelyev, *Handbook on the Physics and Chemistry of Rare Earths Including Actinides*, **2013**, 43, 159–212.
[40] L. K. Jakobsson, G. Tranell, I.-H. Jung, *Metall. Mater. Trans. B* **2017**, *48*, 60–72.
[41] M. Orefice, K. Binnemans, T. Vander Hoogerstraete, *RSC Adv.* **2018**, *8*, 9299–9310.
[42] M. Orefice, A. Van den Bulck, B. Blanpain, K. Binnemans, *J. Sustain. Metall.* **2020**, *6*, 91–102.
[43] J. A. Bogart, C. A. Lippincott, P. J. Carroll, E. J. Schelter, *Angew. Chem. Int. Ed.* **2015**, *54*, 8222–8225.
[44] B. E. Cole, T. Cheisson, J. J. M. Nelson, R. F. Higgins, M. R. Gau, P. J. Carroll, E. J. Schelter, *ACS Sustainable Chem. Eng.* **2020**, *8*, 14786–14794.
[45] A. Falco, M. Neri, M. Melegari, L. Baraldi, G. Bonfant, M. Tegoni, A. Serpe, L. Marchiò, *Inorg. Chem.* **2022**, *61*, 16110–16121.
[46] J. G. O'Connell-Danes, B. T. Ngwenya, C. A. Morrison, J. B. Love, *Nat. Commun.* **2022**, *13*, 4497.
[47] D. N. Mangel, G. J. Juarez, S. H. Carpenter, A. Steinbrueck, V. M. Lynch, J. Yang, A. C. Sedgwick, A. Tondreau, J. L. Sessler, *J. Am. Chem. Soc.* **2023**, *145*, 22206–22212.
[48] H. Ya Gao, W. Li Peng, P. Pan Meng, X. Feng Feng, J. Qiang Li, H. Qiong Wu, C. Sheng Yan, Y. Yang Xiong, F. Luo, *Chem. Commun.* **2017**, *53*, 5737–5739.
[49] A. Masuya-Suzuki, K. Hosobori, R. Sawamura, Y. Abe, R. Karashimada, N. Iki, *Chem. Commun.* **2022**, *58*, 2283–2286.
[50] P. Di Bernardo, A. Melchior, M. Tolazzi, P. L. Zanonato, *Coord. Chem. Rev.* **2012**, *256*, 328–351.
[51] M. J. Polinski, D. J. Grant, S. Wang, E. V. Alekseev, J. N. Cross, E. M. Villa, W. Depmeier, L. Gagliardi, T. E. Albrecht-Schmitt, *J. Am. Chem. Soc.* **2012**, *134*, 10682–10692.
[52] X. Yin, Y. Wang, X. Bai, Y. Wang, L. Chen, C. Xiao, J. Diwu, S. Du, Z. Chai, T. E. Albrecht-Schmitt, S. Wang, *Nat. Commun.* **2017**, *8*, 14438.
[53] R. Van Deun, P. Fias, P. Nockemann, A. Schepers, T. N. Parac-Vogt, K. Van Hecke, L. Van Meervelt, K. Binnemans, *Inorg. Chem.* **2004**, *43*, 8461–8469.
[54] F. Artizzu, L. Marchiò, M. L. Mercuri, L. Pilia, A. Serpe, F. Quochi, R. Orrù, F. Cordella, M. Saba, A. Mura, G. Bongiovanni, P. Deplano, *Adv. Funct. Mater.* **2007**, *17*, 2365–2376.
[55] N. F. Ghazali, K. R. Vignesh, W. Phonsri, K. S. Murray, P. C. Junk, G. B. Deacon, D. R. Turner, *Dalton Trans.* **2022**, *51*, 18502–18513.
[56] V. Prachayasittikul, V. Prachayasittikul, S. Prachayasittikul, S. Ruchirawat, *Drug Des. Dev. Ther.* **2013**, *7*, 1157.
[57] V. Oliveri, G. Vecchio, *Eur. J. Med. Chem.* **2016**, *120*, 252–274.
[58] G. Bissani, P. Carolina, A. Diogo, *ChemistrySelect* **2023**, *8*, 1–16.

[59] W.-Q. Ding, B. Liu, J. L. Vaught, H. Yamauchi, S. E. Lind, *Cancer Res.* **2005**, *65*, 3389–3395.
[60] H. Jiang, J. E. Taggart, X. Zhang, D. M. Benbrook, S. E. Lind, W.-Q. Ding, *Cancer Lett.* **2011**, *312*, 11–17.
[61] L. J. Diorazio, D. R. J. Hose, N. K. Adlington, *Org. Process Res. Dev.* **2016**, *20*, 760–773.
[62] C. Capello, U. Fischer, K. Hungerbühler, *Green Chem.* **2007**, *9*, 927.
[63] F. Jian, Y. Wang, L. Lu, X. Yang, X. Wang, S. Chantrapromma, H.-K. Fun, I. A. Razak, *Acta Crystallogr. Sect. C Cryst. Struct. Commun.* **2001**, *57*, 714–716.
[64] B. Li, J. Zhang, X. Zhang, J. Tian, G. Huang, *Inorg. Chim. Acta* **2011**, *366*, 241–246.
[65] K. Binnemans, P. McGuiness, P. T. Jones, *Nat. Rev. Mater.* **2021**, *6*, 459–461.
[66] Z. Pang, L. Lin, F. Wang, S. Fang, Y. Dai, S. Han, *Appl. Phys. Lett.* **2011**, *99*, 153306.
[67] A. Alemayehu, A. Zakharanka, V. Tyrpekl, *ACS Omega* **2022**, *7*, 12288–12295.
[68] F. Roschangar, R. A. Sheldon, C. H. Senanayake, *Green Chem.* **2015**, *17*, 752–768.
[69] F. P. Byrne, S. Jin, G. Paggiola, T. H. M. Petchey, J. H. Clark, T. J. Farmer, A. J. Hunt, C. Robert McElroy, J. Sherwood, *Sustain. Chem. Process.* **2016**, *4*, 7.
[70] A. Gałuszka, Z. M. Migaszewski, P. Konieczka, J. Namieśnik, *TrAC Trends Anal. Chem.* **2012**, *37*, 61–72.
[71] P. Lei, S. Ayton, A. I. Bush, *J. Biol. Chem.* **2021**, *296*, 100105.
[72] L. De Almeida, S. Grandjean, N. Vigier, F. Patisson, *Eur. J. Inorg. Chem.* **2012**, *2012*, 4986–4999.
[73] R. G. Parr, *Horizons Quantum Chem.* **1980**, 5–15.
[74] Frisch, M.J., Trucks, G.W., Schlegel, H.B., Scuseria, G.E., Robb, M.A., Cheeseman, J.R.; Scalmani, G.; Barone, V.; Petersson, G.A.; Nakatsuji, H.; Li, X.; Caricato, M.; Marenich, A.V.; Bloino, J., Janesko, B.G., Gomperts, R., Mennucci, B., Hratchian, H.P., Ortiz, J.V., Izmaylov, A.F., Sonnenberg, J.L., Williams-Young, D., Ding, F., Lipparini, F., Egidi, F., Goings, J., Peng, B., Petrone, A., Henderson, T., Ranasinghe, D., Zakrzewski, V.G., Gao, J., Rega, N., Zheng, G., Liang, W., Hada, M., Ehara, M., Toyota, K., Fukuda, R., Hasegawa, J., Ishida, M., Nakajima, T., Honda, Y., Kitao, O., Nakai, H., Vreven, T., Throssell, K., Montgomery Jr., J.A., Peralta, J.E., Ogliaro, F., Bearpark, M.J., Heyd, J.J., Brothers, E.N., Kudin, K.N., Staroverov, V.N., Keith, T.A., Kobayashi, R., Normand, J., Raghavachari, K., Rendell, A.P., Burant, J.C., Iyengar, S.S., Tomasi, J., Cossi, M., Millam, J.M., Klene, M., Adamo, C., Cammi, R., Ochterski, J.W., Martin, R.L., Morokuma, K., Farkas, O., Foresman, J.B., Fox, D.J., Gaussian 16 (**2016**), Revision B.01, Gaussian, Inc., Wallingford CT.
[75] J. Da Chai, M. Head-Gordon, *Phys. Chem. Chem. Phys.* **2008**, *10*, 6615–6620.
[76] S. Grimme, *J. Comput. Chem.* **2006**, *27*, 1787–1799.
[77] W. J. Hehre, R. Ditchfield, J. A. Pople, *J. Chem. Phys.* **2003**, *56*, 2257–2261.
[78] A. Bergner, M. Dolg, W. Küchle, H. Stoll, H. Preuß, *Mol. Phys.* **1993**, *80*, 1431–1441.
[79] M. Dolg, H. Stoll, A. Savin, H. Preuss, *Theor. Chim. Acta* **1989**, *75*, 173–194.
[80] B. Mennucci, J. Tomasi, *J. Chem. Phys.* **1997**, *106*, 5151–5158.
[81] L. Maron, O. Eisenstein, *J. Phys. Chem. A* **2000**, *104*, 7140–7143.
[82] B. M. Örnemark, U. Örnemark, *Eurachem Guide: The Fitness for Purpose of Analytical Methods – A Laboratory Guide to Method Validation and Related Topics, (2nd Ed.).* **2014**, 1–62.
[83] P. Dangelo, A. Zitolo, V. Migliorati, G. Chillemi, M. Duvail, P. Vitorge, S. Abadie, R. Spezia, *Inorg. Chem.* **2011**, *50*, 4572–4579.
[84] R. Van Deun, P. Fias, P. Nockemann, A. Schepers, T. N. Parac-Vogt, K. Van Hecke, L. Van Meervelt, K. Binnemans, *Inorg. Chem.* **2004**, *43*, 8461–8469.
[85] N. F. Chilton, G. B. Deacon, O. Gazukin, P. C. Junk, B. Kersting, S. K. Langley, B. Moubaraki, K. S. Murray, F. Schleife, M. Shome, D. R. Turner, J. A. Walker, *Inorg. Chem.* **2014**, *53*, 2528–2534.
[86] E. V. Baranov, G. K. Fukin, T. V. Balashova, A. P. Pushkarev, I. D. Grishin, M. N. Bochkarev, *Dalton Trans.* **2013**, *42*, 15699–15705.
[87] S. G. Leary, G. B. Deacon, P. C. Junk, *Zeitschrift für Anorg. und Allg. Chemie* **2005**, *631*, 2647–2650.
[88] F. Artizzu, P. Deplano, L. Marchiò, M. L. Mercuri, L. Pilia, A. Serpe, F. Quochi, R. Orrù, F. Cordella, F. Meinardi, R. Tubino, A. Mura, G. Bongiovanni, *Inorg. Chem.* **2005**, *44*, 840–842.
[89] L. P. E. Silina, Yu. Bankovsky, V. Belsky, J. Lejejs, *Latv. Kim. Z.* **1997**, *4*, 89–90.
[90] F. Artizzu, F. Quochi, L. Marchiò, R. F. Correia, M. Saba, A. Serpe, A. Mura, M. L. Mercuri, G. Bongiovanni, P. Deplano, *Chem. Eur. J.* **2015**, *21*, 3882–3885.
[91] R. D. Shannon, *Acta Crystallogr. Sect. A* **1976**, *32*, 751–767.
[92] D. J. C. Constable, A. D. Curzons, V. L. Cunningham, *Green Chem.* **2002**, *4*, 521–527.
[93] R. A. Sheldon, *Green Chem.* **2007**, *9*, 1273–1283.
[94] U. Bruker, *APEXIV. Bruker AXS Inc.*, Madison, Wisconsin, USA, **2012**.
[95] Y. chun Liu, Z. yin Yang, *Eur. J. Med. Chem.* **2009**, *44*, 5080–5089.
[96] A. Poater, B. Cosenza, A. Correa, S. Giudice, F. Ragone, V. Scarano, L. Cavallo, *Eur. J. Inorg. Chem.* **2009**, 1759–1766.
[97] L. Falivene, Z. Cao, A. Petta, L. Serra, A. Poater, R. Oliva, V. Scarano, L. Cavallo, *Nat. Chem.* **2019**, *11*, 872–879.
[98] L. Krause, R. Herbst-Irmer, G. M. Scheldrick, D. Stalke,, *J. Appl. Cryst.* **2015**, *48, 3–10*.
[99] G. M. Sheldrick, *Acta Crystallogr. Sect. A Found. Crystallogr.* **2015**, *71*, 3–8.
[100] A. L. Spek, *Acta Crystallogr. Sect. C Struct. Chem.* **2015**, *71*, 9–18.
[101] O. V. Dolomanov, L. J. Bourhis, R. J. Gildea, J. A. K. Howard, H. Puschmann, *J. Appl. Crystallogr.* **2009**, *42*, 339–341.
[102] M. Sevvana, M. Ruf, I. Usón, G. M. Sheldrick, R. Herbst-Irmer, *Acta Crystallogr. Sect. D Struct. Biol.* **2019**, *75*, 1040–1050.
[103] C. F. Macrae, P. R. Edgington, P. McCabe, E. Pidcock, G. P. Shields, R. Taylor, M. Towler, J. Van De Streek, *J. Appl. Crystallogr.* **2006**, *39*, 453–457.

Manuscript received: February 10, 2024
Revised manuscript received: May 23, 2024
Accepted manuscript online: May 24, 2024
Version of record online: July 8, 2024